

Energy Relaxation Dynamics of Excited Triplet States of Directly Linked Zn(II)Porphyrin Arrays[†]

Nam Woong Song,[‡] Hyun Sun Cho, Min-Chul Yoon, Naoki Aratani,[§] Atsuhiko Osuka,^{§,*} and Dongho Kim*

[‡]Laser Metrology Laboratory, Korea Research Institute of Standards and Science, Taejeon 305-600, Korea
Center for Ultrafast Optical Characteristics Control and Department of Chemistry,
Yonsei University, Seoul 120-741, Korea

[§]Department of Chemistry, Graduate School of Science, Kyoto University, Kyoto 606-8502, Japan
Received October 5, 2001

The energy relaxation dynamics of the lowest excited singlet and triplet states of the Zn(II)porphyrin monomer and its directly linked arrays were comparatively investigated with increasing the number of porphyrin moieties. While the fluorescence decay rates and quantum yields of the porphyrin arrays increased with the increase of porphyrin units, their triplet-triplet (T-T) absorption spectra and decay times remained almost the same. The difference in the trends of energy relaxation dynamics between the excited singlet and triplet states has been discussed in view of the electronic orbital configurations.

Keywords : Triplet state, Zn(II)porphyrin array, Flash photolysis.

Introduction

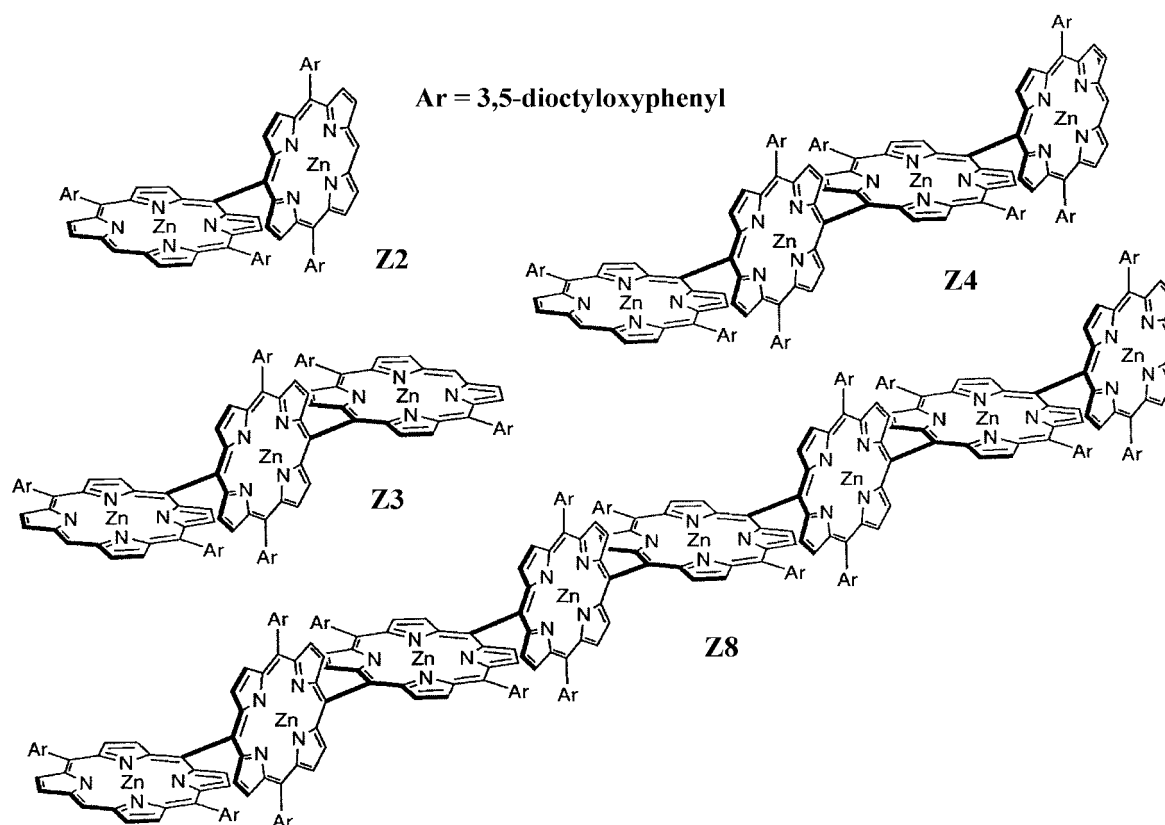
Natural light-gathering arrays have long been an ideal target to elicit molecular design for the fabrication of molecular photonic devices. As a result of continuing efforts to realize the mimicry of solar energy harvesting complexes, various types of covalently linked arrays of metalloporphyrins have been designed and synthesized with the goal of applying these oligomers to molecular photonic devices and artificial biomimetic light-harvesting array systems.¹⁻⁹ The recent progress in synthesizing capabilities of various porphyrin arrays raises a fundamental question regarding the photophysical properties and molecular architecture relationship such as energy migration/gradient. The numbers of pigments, spectral and electronic properties of pigments, and linkage structure have a strong influence on the overall photophysical properties of porphyrin oligomers.

More specifically, the direct *meso-meso* connection with ~8.4 Å center-to-center distance results in exceptionally strong electronic coupling between the adjacent porphyrin units to exhibit a large exciton coupling energy of approximately 4,300 cm⁻¹ derived from the plots of the exciton splitting in Soret transitions.¹⁰ On the contrary, the Q bands of the directly linked porphyrin arrays are much less perturbed as evidenced by smaller red shift presumably due to much weaker oscillator strength of Q transition. This unique property in these types of porphyrin arrays deserves much attention especially in the exciton coupling in relation to the dihedral angle between the adjacent porphyrin moieties. Up to now, the construction of this connection in long linear porphyrin arrays is known to lack synthetic control. Very recently it became possible to connect the porphyrin molecules directly up to one hundred twenty eight units.¹¹ A

directly linked bridge enforces a large dihedral angle between each constituent; the calculated minimum energy torsional angle for this species resides at 90 ± 15 degree at ambient temperature. While the nearly orthogonal orientation of the (porphinato)-zinc(II) units in the arrays restricts inter-ring ground-state conjugation, it allows for mixing of the electronic states of each monomer by excitonic interactions. It is to be noted that the absorption bands for the Q-states resemble those of an isolated porphyrin monomer, indicative of the fact that the lowest singlet electronic excited states of the directly linked dimer are weakly-coupled and localized, which preserve the x-y degeneracy associated with the emitting states of each monomer. This observation also indicates that the dominant low-energy component in the solution spectrum arises from an orthogonal structure in addition to the existence of vibronic states. Equally important, the direct linkage of porphyrin units definitely provides a rigid structure which is important to minimize the heterogeneity of the molecular wires mainly induced by the dihedral angle distribution between the adjacent porphyrin units especially as the length of the molecular wires becomes longer. The heterogeneity of the molecular wires can be minimized in the directly linked porphyrin arrays due to the maintenance of the orthogonality between the adjacent porphyrins.

In the present work, the series of directly linked Zn(II)-porphyrin arrays starting with dimer (Z2) along with constituent monomer (Z1) were employed to investigate the differences in the photophysical properties depending on the number of porphyrin units in molecular arrays (Scheme 1). Absorption, emission and excited triplet state absorption spectra were systematically observed with increasing the number of porphyrin units. The deactivation processes of the excited singlet and triplet states of the porphyrin arrays were also observed by using the fluorescence decay and nano-second laser flash photolysis measurements.

[†]This work has been contributed in commemoration of the retirement of Professor Kyung Hoon Jung at KAIST.



Scheme 1. Molecular geometry of the Zn(II)porphyrin arrays.

Materials and Methods

Zn(II) 5,15-bis(3,5-dioctyloxyphenyl)porphyrin monomer (Z1), and its *meso, meso*-linked porphyrin oligomers such as dimer (Z2), trimer (Z3), hexamer (Z6), and dodecamer (Z12) were synthesized through repetitive Ag(I)-promoted *meso-meso* coupling reactions. The recycling GPC-HPLC was used for product separation. MALDI-TOF (time-of-flight) mass and ^1H NMR spectra were observed for product characterization. The spectroscopic grade tetrahydrofuran (THF) and toluene were used as solvent for all experiments. The absorption spectra were recorded by using a Varian Cary 3 spectrophotometer. The fluorescence and phosphorescence measurements were performed on a scanning SLM-AMINCO 4800 fluorometer.

The fluorescence decay time measurements were carried out by using time correlated single photon counting (TCSPC) method.¹² The excitation pulses at 410 nm were obtained from a femtosecond Ti:sapphire laser (Coherent, MIRA) with an average power of 600 mW at 820 nm. The pump pulses at desired wavelength were generated by frequency doubling with a β -BBO crystal. The emission was collected at 45-degree angle with respect to the excitation laser beam by 5- and 25-cm focal length lenses, focused onto a monochromator (Jobin-Yvon HR320), and detected with a microchannel plate photomultiplier tube (Hamamatsu R2809U). The signal was amplified by a wideband amplifier (Philip Scientific), sent to a Quad constant fraction discriminator

(Tennelec), a time-to-amplitude converter (Tennelec), a counter (Ortec), and a multichannel analyzer (Tennelec/Nucleus), and stored in a computer. The time dependent anisotropy decay was obtained by using the polarizer and depolarizer before the detection system.

A detailed schematic diagram of the experimental setup for the nanosecond laser flash photolysis can be found elsewhere.¹³ A brief description will be given here. An excitation pulse of 416 nm was generated by using the stimulated Stokes Raman process of the third harmonic (355 nm) output from a Q-switched Nd:YAG laser (Continuum SLI-20) in a Raman shifter containing H_2 gas of 1 atm. A pair of Pellin-Broca prisms and pinholes of 5 mm in diameter were used to clearly separate the 416 nm laser pulse from the other Stokes and *anti*-Stokes shifted laser lines. The time duration of the excitation pulse was *ca.* 6 ns, and the pulse energy was *ca.* 2 mJ. A CW tungsten-halogen lamp (150 W) was used as the probe light source for transient absorption measurement. The probe light was collimated on the sample cell and then spectrally resolved by using a 320 mm monochromator (Jobin-Yvon HR320) equipped with a 600 grooves/mm grating after passing through the sample. The spectral resolution was about 3 nm for transient absorption experiment. The light signal was detected by using a head-on type photomultiplier tube (Hamamatsu, model R943-02) which has relatively flat response curve for the photon wavelength from UV to near IR region. The output signal from the PMT was recorded

with a Boxcar signal averager (Stanford Research System SR250) for the spectrum measurement or a 500 MHz digital storage oscilloscope (DSO) (Hewlett-Packard HP54616B) for the temporal profile measurement. Digitized signal in the Boxcar or DSO was transferred and stored in a personal computer.

Sample solutions were prepared by dissolving the samples in toluene. The sample concentrations were adjusted to be *ca.* 1.5–2.0 in absorbance at 416 nm. The sample solution was circulated from a bottle (500 mL in volume) to a fluorometer quartz cuvette of 10 mm in pathlength (Flow type, Helma QS 1.0) to minimize the sample degradation in the photolysis cell.

Results and Discussion

Absorption spectra. It is well established that the absorption spectrum of porphyrin molecules in the visible and near-UV wavelength range can be divided into two transitions.^{14,15} The upper transition is labeled as B- or Soret band and the lower one as Q-band. Since the excited electronic states corresponding to both B- and Q-bands are of E_u symmetry, they consist of two pairs of degenerate states which are usually called as B_x , B_y and Q_x , Q_y due to the orthogonality of each transition dipole.¹⁴ The absorption spectra of Z1 and its directly linked arrays (Z2, Z3, Z6 and Z12) are shown in Figure 1. The spectral intensities were normalized at the absorption maxima around 413 nm which corresponds to the split Soret band at high energy side. While the Soret band in the absorption spectrum of Z1 exhibited a vibronic progression (1170 cm^{-1}) with a narrow spectral bandwidth (*ca.* 3 nm), the absorption spectra of the porphyrin arrays did not show any distinct vibronic structures in the Soret band region with relatively broad bandwidths ($> 15\text{ nm}$). Furthermore, the *meso-meso* coupled arrays displayed split Soret bands due to exciton coupling as reported previously.^{11,16,17} With an increase in the number of porphyrin units, the exciton split Soret band was shifted to

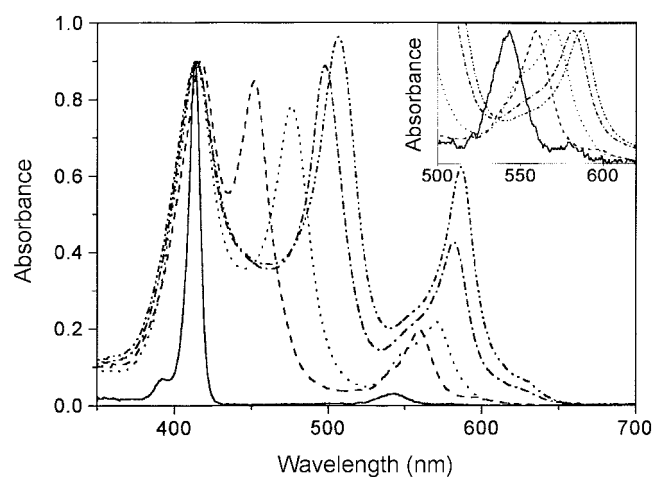
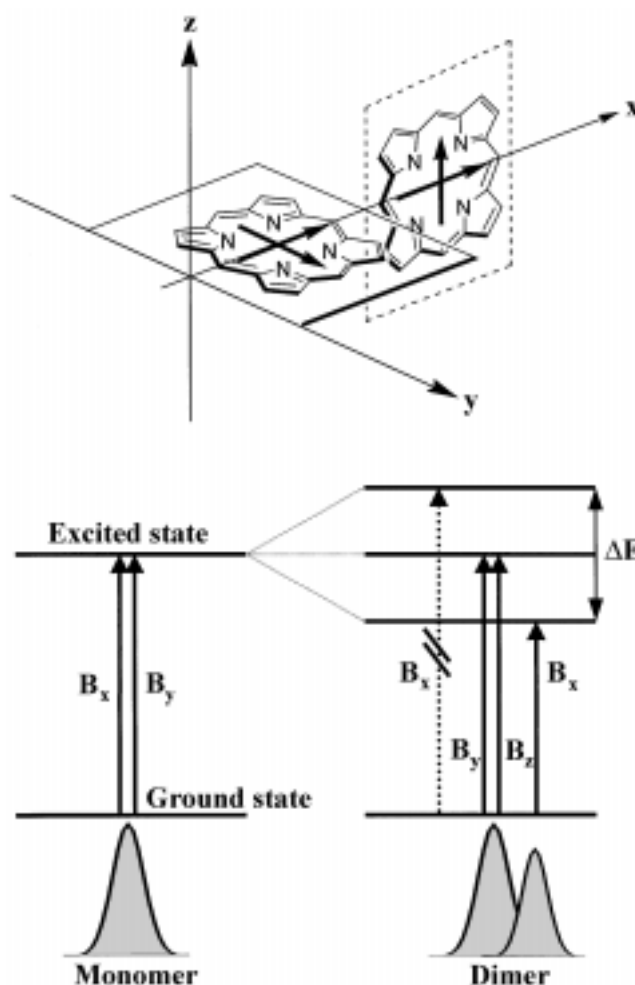


Figure 1. The ground-state absorption spectra of the porphyrin arrays in THF; Z1 (—), Z2 (---), Z3 (···), Z6 (— · —) and Z12 (— · — · —). Inset shows the normalized Q-band absorptions.

longer wavelength resulting in a progressive increase of the splitting energy, while the Soret band at shorter wavelength remained nearly at the same position (*ca.* 413 nm). The increment of the splitting energy became smaller as the number of porphyrin moieties increased over six. The relative intensities of the split Soret bands also depend on the number of porphyrin units; the intensity of lower energy bands becomes stronger relative to that of high energy bands. The relative intensities of Q-bands compared with those of the high energy Soret bands also largely increased with the addition of porphyrin moieties. On the other hand, the spectral changes in the Q-band region are modest with gradual red-shift compared with the exciton split Soret bands (Inset of Figure 1). The red-shift of the Q-band absorption also shows saturation as the number of porphyrin moieties increased over six.

The systematic spectral changes of the Soret bands can be explained in terms of the simple point-dipole exciton coupling theory developed by Kasha.^{10,18} As mentioned above, the Soret band of Zn(II)porphyrin has two perpendicular components of B_x and B_y which are degenerate. In the porphyrin arrays, however, they couple differently as shown in Scheme



Scheme 2. Coupling of the two perpendicular electronic transition dipoles in the orthogonal geometry of Zn(II)porphyrin dimer.

2. In case of Z2, only one component, *e.g.* B_x transitions, is parallel, but the other dipole interactions should be zero due to the orthogonal conformation of Z2 which has been predicted to be the most stable on the basis of AM1 calculation.¹⁰ Unperturbed Soret transitions observed at *ca.* 413 nm for all the arrays (Z2 to Z12) suggest an orthogonal conformation. Transitions are allowed to the lower energy of the two B_x states and the two unperturbed transitions B_y and B_z . Thus, the Soret band of Z2 is split into a red-shifted B_x component and unperturbed B_y , B_z components (Scheme 2).

According to the four-orbital model, the low-lying (π, π^*) excited states of porphyrins can be described in terms of the transitions between two highest occupied molecular orbitals (HOMO's), $a_{2u}(\pi)$ and $a_{1u}(\pi)$, and two degenerate lowest unoccupied molecular orbitals (LUMO's), $e_g(\pi^*)$. For the porphyrin ring, the lowest singlet excited configurations, $a_{2u}(\pi), e_g(\pi^*)$ and $a_{1u}(\pi), e_g(\pi^*)$, are nearly degenerate, and as a consequence there is a strong electronic interaction between them.^{14,15,19,20} The resulting resonance yields the relatively weak visible Q-band, in which the transition dipoles of the two configurations nearly cancel, and the intense Soret band, in which the transition dipoles of the two configurations add. Thus, in reality the Q band of porphyrin monomer borrows its intensity from the B band through vibronic coupling. In the cases of porphyrin arrays, the existence of exciton split B bands between unshifted monomeric B bands and Q bands reduces the energy difference between B and Q bands, which results in an increase in intensity borrowing of Q bands from B bands. Therefore the intensities of Q bands of porphyrin arrays increase in parallel with an increase in the exciton splitting as the number of porphyrin units increases in the porphyrin arrays.

Fluorescence and phosphorescence spectra. The steady-state fluorescence spectra of Z1 and its arrays according to the relative intensity scale are displayed in Figure 2 and the photophysical parameters of the porphyrin arrays are summarized in Table 1. Z1 exhibits two-peak emission (584 and 633 nm) characteristic of Zn(II)porphyrin and Z2 shows a red-shifted and broader fluorescence spectrum. The fluore-

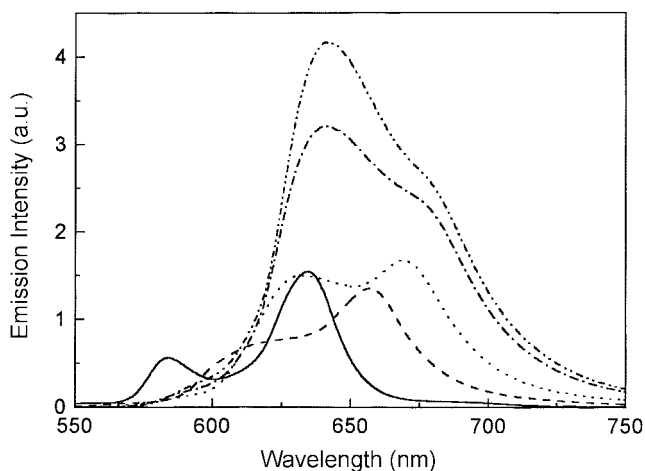


Figure 2. The steady-state fluorescence spectra of the porphyrin arrays in THF; Z1 (—), Z2 (---), Z3 (....), Z6 (-.-.-) and Z12 (-.-.-).

Table 1. Photophysical properties of the Zn(II)porphyrin monomer and arrays

	Φ_F	τ_F (ns) ^d	$\tau_{F,0}$ (ns)	$\lambda_{p,max}$ (nm) ^b	$\lambda_{T-T,max}$ ^c (nm)	τ_T (μ s) ^d
Z1	0.019	2.64	139	743	825	632
Z2	0.027	1.94	72	760	820	689
Z3	0.041	1.83	45	773	825	673
Z6	0.064	1.66	33	781	830	661
Z12	0.068	1.46	21	785	825	675

^aFluorescence lifetime measured at the emission maximum. ^bThe peak wavelength of the phosphorescence. ^cThe peak wavelength of the T-T absorption. ^dTriplet state lifetime measured at 825 nm.

scence spectra of the longer arrays (Z3-Z12) are observed in nearly the same region as the two bands at *ca.* 15600 cm^{-1} (640 nm) and *ca.* 15000 cm^{-1} (667 nm). The relative fluorescence quantum yields determined with respect to $\phi_F = 0.03$ of Zn(II)TPP²¹ increased up to Z12 with the increase of the number of porphyrin units. The natural radiative lifetimes of the porphyrin arrays were also obtained according to the relationship of $\tau_0 = \tau/\Phi$ where τ_0 , τ and Φ are natural radiative lifetimes, fluorescence lifetimes and fluorescence quantum yields of the porphyrin arrays, respectively. The increase of relative fluorescence quantum yield and radiative transition rate was retarded as the number of porphyrin moieties increased over six. The radiative coherence length of the porphyrin arrays investigated in this work has been estimated to be 6-8 porphyrin units based on the observation of radiative lifetime and spectral changes in the exciton split band.²⁰ The radiative transition rate of excitons is expected to be proportional to the coherent length (N units) and the radiative transition rate of monomer, *i.e.* $k_0 = Nk_{0,m}$,²²⁻²⁴ which means that the oscillator strength of the radiative transition increases as the coherent length becomes longer.

Phosphorescence spectra of porphyrin monomer and arrays were observed at 77 K as shown in Figure 3 with normalized intensities at the emission maxima. There was no vibronic structure in the phosphorescence spectra of the porphyrin arrays. Only a gradual red-shift of the emission maximum

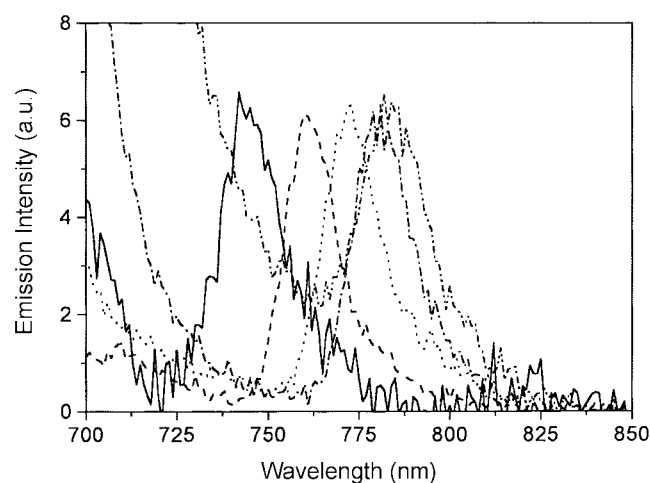


Figure 3. The normalized steady-state phosphorescence spectra of the porphyrin arrays at 77 K; Z1 (—), Z2 (---), Z3 (....), Z6 (-.-.-) and Z12 (-.-.-).

was observed with a retardation in the arrays over six units. It is notable to observe that the T_1 - S_0 energy difference of the porphyrin arrays was reduced while the S_1 - S_0 energy difference was not much affected by the increase of the number of porphyrin units as revealed in the fluorescence spectra of the porphyrin arrays.

Triplet state absorption spectra. The triplet state absorption spectrum of Zn(II)porphyrin is generally composed of two bands; one lies in the visible region and the other in the near-infrared (IR) region.^{25,26} While the near-infrared absorption in the triplet state corresponds to the transition between two states with singly excited configurations [$a_{1u}(\pi), e_g(\pi^*) \rightarrow a_{1u}(\pi), b_{2u}(\pi^*)$ or $a_{2u}(\pi), e_g(\pi^*) \rightarrow a_{2u}(\pi), b_{1u}(\pi^*)$], the visible absorption is known as due to the transition from the lowest excited state with singly excited configuration to the higher excited state with doubly excited configurations [$a_{1u}(\pi), e_g(\pi^*)$ or $a_{2u}(\pi), e_g(\pi^*) \rightarrow a_{1u}(\pi), a_{2u}(\pi), e_g^2(\pi^*)$].²⁶⁻²⁸ We have measured the triplet state absorption spectra of Zn(II) 5,15-bis(3,5-dioctyloxyphenyl) porphyrin monomer (Z1) and its *meso-meso* linked array compounds (Z2, Z3, Z6, and Z12) to investigate the change in the triplet state absorption spectra and their dynamics along with the increase of porphyrin moieties in the arrays.

The triplet-triplet (T-T) absorption spectra of porphyrin monomer and arrays were observed at 5 μ s delay (Figure 4). The T-T absorption spectrum of Z1 showed a characteristic feature arising from the $^3(\pi, \pi^*)$ states of Zn(II)porphyrins. The absorption spectrum is composed of visible and near-IR bands. Since the visible absorption bands in the porphyrin arrays were largely perturbed by the exciton split band, we only observed the near-IR absorption bands in the T-T absorption of the porphyrin arrays. It is generally observed that the vibronic absorption band at the wavelength of 1400-1500 cm^{-1} above the main near-IR absorption peak appears in the triplet state absorption of Zn(II)porphyrins. In the triplet state absorption spectrum of Z1, we could also observe the dual bands in the near-IR region having maxima

at 735 and 825 nm, respectively, which corresponds to the energy difference of *ca.* 1480 cm^{-1} . This spacing of 1400-1500 cm^{-1} is similar to the vibrational spacing normally found in the emission from the $^1(\pi, \pi^*)$ and $^3(\pi, \pi^*)$ states of metalloporphyrins. This feature is known to be insensitive to the peripheral substituents on the porphyrin macrocycle or to the electronic configuration of the central metal.²⁷

The triplet state absorption spectra of the porphyrin arrays (Z2, Z3, Z6, and Z12) were almost the same without any vibronic structure (Figure 4). The lack of the vibronic structure in the T-T absorption spectra of the porphyrin arrays might be attributable to the increased number of upper electronic states with the linkage of porphyrin moieties. The Soret band of the porphyrin arrays also exhibited broad and structureless feature while the absorption spectrum of the monomer showed distinct vibronic bands. It is notable that the T-T absorption maxima of the porphyrin monomer (Z1) and arrays are almost the same while the T_1 state energies were reduced as the number of porphyrin units increased as revealed from the gradual red-shift of the phosphorescence spectra. Since the near-IR absorption bands of Zn(II)porphyrins correspond to the transition of $a_{2u}(\pi), e_g(\pi^*) \rightarrow a_{2u}(\pi), b_{1u}(\pi^*)$, we can expect that the energy of the excited triplet states in the porphyrin arrays corresponding to the $a_{2u}(\pi), b_{1u}(\pi^*)$ triplet state of monomer is reduced with the same quantity as the T_1 state energy stabilization by the linkage of porphyrin moieties. The triplet state lifetimes of the porphyrin monomer and arrays were almost the same around 670 μ s (Table 1 and Inset of Figure 4), while the S_1 state lifetimes were reduced as the number of porphyrin units was increased. As mentioned above, the S_1 states of Zn(II)porphyrin have $a_{1u}(\pi), e_g(\pi^*)$ and $a_{2u}(\pi), e_g(\pi^*)$ configurations which are nearly degenerate and mix each other. On the contrary, the T_1 states of porphyrins have either $a_{1u}(\pi), e_g(\pi^*)$ or $a_{2u}(\pi), e_g(\pi^*)$ orbital configuration which does not mix due to the symmetry. Thus the T_1 state of meso-phenyl substituted Zn(II)porphyrins should possess $a_{2u}(\pi), e_g(\pi^*)$ configuration because a_{2u} orbital is located higher than a_{1u} orbital in this type of porphyrins. The triplet state Raman spectra of Zn(II)TPP reported by Walters *et al.*²⁹ and Reed *et al.*³⁰ revealed relatively small frequency shift along with phenyl mode enhancement in the triplet state Raman spectrum. The phenyl mode enhancement is attributed to the increase of Franck-Condon overlap between porphyrin $e_g(\pi^*)$ and phenyl π^* orbital excitation in the T_1 - T_n electronic transition around 460 nm. Thus, in the triplet (π, π^*) state the configuration interaction manifests itself in the Jahn-Teller effect. Therefore, the asymmetric modes provide distortion coordinates appropriate for the Jahn-Teller effect. The relatively small frequency shift in the triplet state Raman spectra of Zn(II)TPP indicates that the electronic transition of $a_{2u}(\pi), e_g(\pi^*)$ in the triplet state results in negligible change in the triplet state geometry. Raman frequencies for cationic (one electron is removed from a_{2u} orbital) and anionic (one electron is added into e_g orbital) forms of Zn(II)TPP give rise to opposite frequency shift for some high-frequency Raman modes. This feature also indicates that the electronic

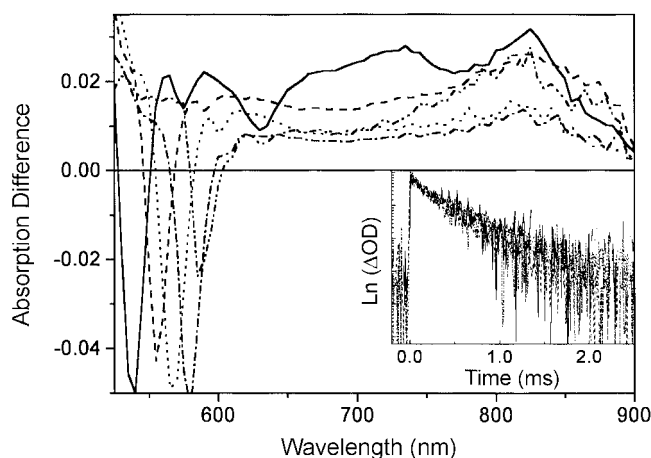


Figure 4. The T-T absorption spectra of the porphyrin arrays in toluene; Z1 (—), Z2 (---), Z3 (....), Z6 (-.-.-) and Z12 (-.-.-). Inset shows the normalized decay profile of the T-T absorption at 825 nm.

nature of the T_1 state of Zn(II)porphyrins remains as unmixed electronic configuration of $a_{2u}(\pi), e_g(\pi^*)$. Since the electronic nature of the T_1 states of the porphyrin arrays should remain the same as $a_{2u}(\pi), e_g(\pi^*)$ configuration, the relaxation dynamics of the T_1 states of the porphyrin arrays are likely governed by the energy gap between T_1 and S_0 states. Thus the triplet state lifetimes of the porphyrin monomer and arrays are expected to be almost unchanged, while the S_1 states with mixed electronic configurations are largely sensitive to the perturbation of electronic configurations by the linkage of porphyrin moieties.

Conclusion

We have observed the absorption, fluorescence, phosphorescence and T-T absorption spectra of Zn(II)porphyrin monomer and its directly linked arrays with increasing the number of porphyrin moieties. The relaxation dynamics of the lowest excited singlet and triplet states were comparatively investigated. In the absorption spectra, *meso-meso* coupled Zn(II)porphyrin arrays displayed split Soret bands which were shifted to longer wavelength with increasing the number of porphyrin units due to exciton coupling. Gradual red-shift in the Q-band absorption and phosphorescence spectra was also observed with the increase of the number of porphyrin moieties. Fluorescence decay rate and quantum yield increased as the length of porphyrin arrays became longer due to larger radiative coherent length of 6-8 porphyrin units. On the other hand, the T-T absorption spectra and their decay times of the porphyrin arrays were almost the same without any vibronic structure. The difference in the trends of the energy relaxation dynamics between the excited singlet and triplet states are attributable to the difference in the electronic configurations between the two states; while the S_1 states of the Zn(II)porphyrin arrays have the mixed electronic orbital configurations of $a_{1u}(\pi), e_g(\pi^*)$ and $a_{2u}(\pi), e_g(\pi^*)$, the T_1 states have $a_{2u}(\pi), e_g(\pi^*)$ orbital configuration which does not mix with $a_{1u}(\pi), e_g(\pi^*)$ due to the symmetry. Thus, the T_1 states of the porphyrin arrays are expected to be less sensitive to the perturbation of electronic states by the linkage of porphyrin moieties than the S_1 states.

Acknowledgment. This work has been financially supported by the National Creative Research Initiatives of the Ministry of Science & Technology of Korea (DK). The work at Kyoto was supported by Grant-in-Aids for Scientific Research from the Ministry of Education, Science, Sports and Culture of Japan and by CREST (Core Research for Evolutional Science and Technology) of Japan Science and

Technology Corporation (JST).

References

- Gouterman, M.; Holten, D.; Lieberman, S. *Chem. Phys.* **1977**, *25*, 139.
- Chang, C. K. *J. Heterocycl. Chem.* **1977**, *14*, 1285.
- Ichimura, K. *Chem. Lett.* **1977**, 641.
- Kagan, N. E.; Mauzerall, D.; Merrifield, R. B. *J. Am. Chem. Soc.* **1977**, *99*, 5484.
- Collman, J. P.; Prodollet, J. W.; Leidner, C. R. *J. Am. Chem. Soc.* **1986**, *108*, 2916.
- Collman, J. P.; Chong, A. O.; Jameson, G. B.; Oakley, R. T.; Rose, E.; Schmittou, E. R.; Ibers, J. A. *J. Am. Chem. Soc.* **1981**, *103*, 516.
- Konishin, S.; Hoshino, M.; Imamura, M. *J. Phys. Chem.* **1982**, *86*, 4888.
- Brookfield, R. L.; Ellul, H.; Harriman, A. *J. Chem. Soc., Faraday Trans. 2* **1985**, *81*, 1837.
- Kadish, K. M.; Moninot, G.; Hu, Y.; Dubois, D.; Ibnlfassi, A.; Barbe, J.-M.; Guillard, R. *J. Am. Chem. Soc.* **1993**, *115*, 8153.
- Kim, Y. H.; Jeong, D. H.; Kim, D.; Jeong, S. C.; Cho, H. S.; Kim, S. K.; Aratani, N.; Osuka, A. *J. Am. Chem. Soc.* **2001**, *123*, 76.
- Aratani, N.; Osuka, A.; Kim, D.; Kim, Y. H.; Jeong, D. H. *Angew. Chem.* **2000**, *39*, 1458.
- Lee, M.; Kim, D. *J. Opt. Soc. Korea* **1990**, *52*, 1.
- Park, Y.-T.; Song, N. W.; Hwang, C.-G.; Kim, K.-W.; Kim, D. *J. Am. Chem. Soc.* **1997**, *119*, 10677.
- Gouterman, M. *J. Chem. Phys.* **1959**, *30*, 1139.
- Spellane, P. J.; Gouterman, M.; Antipas, A.; Kim, S.; Liu, Y. C. *Inorg. Chem.* **1980**, *19*, 386.
- Osuka, A.; Shimidzu, H. *Angew. Chem., Int. Ed. Engl.* **1997**, *36*, 135.
- Yoshida, N.; Shimidzu, H.; Osuka, A. *Chem. Lett.* **1998**, 55.
- Kasha, M.; Rawls, H. R.; El-Bayoumi, M. *Pure Appl. Chem.* **1965**, *11*, 371.
- Gouterman, M. *J. Mol. Spectrosc.* **1961**, *6*, 138.
- Weiss, C.; Kobayashi, H.; Gouterman, M. *J. Mol. Spectrosc.* **1965**, *16*, 415.
- Li, X.-Y.; Czernuszewicz, R. S.; Kincaid, J. R.; Su, Y. O.; Spiro, T. G. *J. Phys. Chem.* **1990**, *94*, 31.
- Kuhn, H. *J. Chem. Phys.* **1970**, *53*, 101.
- de Boer S.; Wiersma, D. A. *Chem. Phys. Lett.* **1990**, *165*, 45.
- Scheblykin, I. G.; Bataiev, M. M.; Van der Auweraer, M.; Vitukhnovsky, A. G. *Chem. Phys. Lett.* **2000**, *316*, 37.
- Pekkarinen, L.; Linschitz, H. *J. Am. Chem. Soc.* **1960**, *82*, 2407.
- Gouterman, M. *J. Chem. Phys.* **1960**, *33*, 1523.
- Rodriguez, J.; Kirmaier, C.; Holten, D. *J. Am. Chem. Soc.* **1989**, *111*, 6500.
- Walters, V. A.; de Paula, J. C.; Jackson, B.; Nutaitis, C.; Hall, K.; Lind, J.; Cardozo, K.; Chandran, K.; Raible, D.; Phillips, C. M. *J. Phys. Chem.* **1995**, *99*, 1166.
- Walters, V. A.; de Paula, J. C.; Babcock, G. T.; Leroi, G. E. *J. Am. Chem. Soc.* **1989**, *111*, 8300.
- Reed, R. A.; Purrello, R.; Prendergast, K.; Spiro, T. G. *J. Phys. Chem.* **1991**, *95*, 9720.